Oligocene climate dynamics

Bridget S. Wade[1]
Grant Institute of Earth Sciences, School of Geosciences, University of Edinburgh, West Mains Road, Edinburgh, UK

Heiko Pälike[2]
Department of Geology and Geochemistry, Stockholm University, Stockholm, Sweden

Received 18 April 2004; revised 30 July 2004; accepted 20 September 2004; published 8 December 2004.

[1] A planktonic and benthic foraminiferal stable isotope stratigraphy of the Oligocene equatorial Pacific (Ocean Drilling Program, Site 1218) was generated at 6 kyr resolution between magnetochrons C9n and C11n.2n (~26.4–30 Ma on a newly developed astronomically calibrated timescale). Our data allow a detailed examination of Oligocene paleoceanography, the evolution of the early cryosphere, and the influence of orbital forcing on glacioeustatic sea level variations. Spectral analysis reveals power and coherency for obliquity (40 kyr period) and eccentricity (~110, 405 kyr) orbital bands, with an additional strong imprint of the eccentricity and 1.2 Myr obliquity amplitude cycle, driving ice sheet oscillations in the Southern Hemisphere. Planktonic and benthic foraminifera $\delta^{18}O$ are used to constrain the magnitude and timing of major fluctuations in ice volume and global sea level change. Glacial episodes, related to obliquity and eccentricity variations, occurred at 29.16, 27.91, and 26.76 Ma, corresponding to glacioeustatic sea level fluctuations of 50–65 m. Alteration of high-latitude temperatures and Antarctic ice volume had a significant impact on the global carbon burial and equatorial productivity, as cyclic variations are also recorded in the carbon isotope signal of planktonic and benthic foraminifera, the water column carbon isotope gradient, and estimated percent carbonate of bulk sediment. We also investigate the implications of a close correspondence between oxygen and carbon isotope events and long-term amplitude envelope extrema in astronomical calculations during the Oligocene, and develop a new naming scheme for stable isotope events, on the basis of the 405 kyr eccentricity cycle count. *INDEX TERMS:* 1620 Global Change: Climate dynamics (3309); 3030 Marine Geology and Geophysics: Micropaleontology; 4556 Oceanography: Physical: Sea level variations; 4267 Oceanography: General: Paleoceanography; 9355 Information Related to Geographic Region: Pacific Ocean; *KEYWORDS:* Oligocene, stable isotopes, ice volume

Citation: Wade, B. S., and H. Pälike (2004), Oligocene climate dynamics, *Paleoceanography*, *19*, PA4019, doi:10.1029/2004PA001042.

1. Introduction

1.1. Oligocene Climate and Unipolar Glaciation

[2] The Oligocene has previously been perceived as an interval of climatic stability, yet the oscillation of the Antarctic ice sheet through the Oligocene gave rise to glacioeusatic sea level variations of up to 100 m [*Miller et al.*, 1987, 1991, 1998; *Pekar and Miller*, 1996; *Pekar et al.*, 2000, 2001]. Documentation of how the climate is influenced by substantial ice volume changes on Antarctica is vital in understanding primary climate processes. However, very little is known about climatic dynamics during this interval of unipolar glaciation and how major fluctuations in Southern Hemisphere ice volume would have propagated through the ocean-atmosphere system.

[3] Here we present a detailed stable isotope record of both planktonic (Figure 1) and benthic foraminifera for a 3.6 Myr interval spanning the early and late Oligocene (26.4 to 30.0 Ma) from the tropical Pacific. These data supply a comprehensive chronology of oceanographic and climatic fluctuations and an isotopic reference curve for the Oligocene Pacific Ocean. Samples were analyzed at a 10 cm resolution giving a sampling frequency of 1 sample/6000 years. This is the highest resolution ever applied over this interval and thus provides unprecedented insights into temperature variability, the carbon cycle major ice volume changes, and their relationship to astronomical cycles.

1.2. Site Description

[4] Ocean Drilling Program (ODP) Leg 199, "The Paleogene Equatorial Transect" drilled 8 sites in the tropical Pacific Ocean (Sites 1215–1222). Site 1218 (8°53.378″N, 135°22.00″W) is located in the eastern equatorial Pacific, in a water depth of 4826 m [*Shipboard Scientific Party*, 2002]. Additional information can be found in the supplementary material[1]. The Oligocene sequence from Site 1218 has a clear magnetostratigraphy and abundant foraminifera through most of the Oligocene. Cyclic variations are evident

[1]Now at School of Earth, Ocean and Planetary Sciences, Cardiff University, Cardiff, UK.

[2]Now at Southampton Oceanography Centre, School of Ocean and Earth Science, Southampton, UK.

0883-8305/04/2004PA001042

[1]Auxiliary material is available at ftp://ftp.agu.org/apend/pa/2004PA001042.

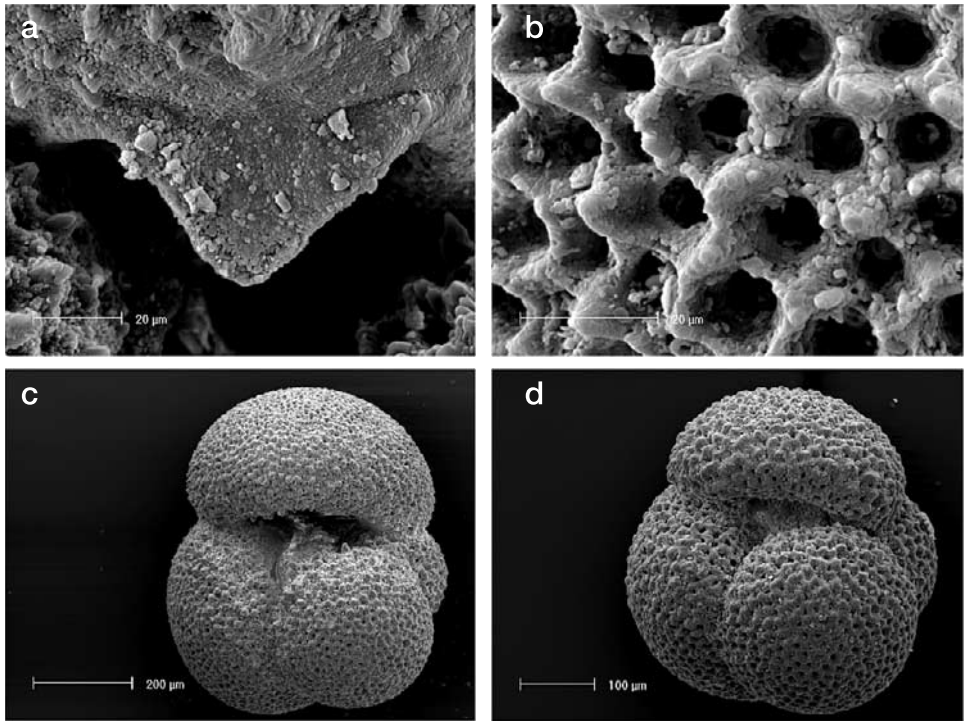

Figure 1. Oligocene planktonic foraminifera from Site 1218 (note changes in scale bar). (a) and (b) Recrystallized test surface of *Dentoglobigerina globularis* from sample 1218B, 15-H-3, 60–62 cm. (c) *Globoquadrina venezuelana*, umbilical view, sample 1218B, 15-H-3, 60–62 cm. (d) *Globoquadrina venezuelana*, umbilical view, sample 1218A, 14-H-4, 50–52 cm.

in sediment color and magnetic susceptibility which reflect orbital variations of solar insolation [*Shipboard Scientific Party*, 2002]. These features, coupled with the high-resolution stable isotope data generated here, allow a detailed examination of the icehouse world of the Oligocene. During the Oligocene, Site 1218 was located at a paleolatitude of 3–4°N of the equator [*Shipboard Scientific Party*, 2002] and thus planktonic foraminiferal stable isotopes provide a record of tropical paleoceanography in the Paleogene Pacific Ocean. Sedimentation rates are high and average 15m Myr^{-1}, which facilitates the development of an orbital-scale stable isotope and physical property stratigraphy.

2. Materials and Methods

[5] The methodology and sample processing are detailed in the supplementary material.

3. Results

3.1. Benthic Foraminifera Oxygen Isotopes

[6] It was found in previous studies that stable isotope measurements from modern benthic foraminifera are not in equilibrium with the surrounding seawater [*Duplessy et al.*, 1970]. Thus it is necessary to use species-specific adjustment factors in order to make data comparable between different benthic species. We adjusted Cibicidoides $\delta^{18}O$ values to seawater equilibrium by adding +0.64‰ [*Shackleton and Opdyke*, 1973]. No correction was applied to $\delta^{13}C$ values. In the following benthic oxygen isotope description, and associated figures, we refer to the adjusted oxygen isotope values.

[7] Benthic foraminifera $\delta^{18}O$ values range between 1.51 and 3.10‰ (Figure 2). The median value of benthic $\delta^{18}O$ values is 2.43‰, with a standard deviation of 0.27‰. These values are similar to previous benthic oxygen isotope measurements from the central equatorial Pacific (DSDP 77, 574). From the early to the late part of the record we observe a general increase toward heavier $\delta^{18}O$ values: a linear regression shows an increase of ~0.4‰ throughout the study interval. High-amplitude variations of $\delta^{18}O$ values (~0.75–1.2‰) generally occur on short eccentricity timescales (80–130 kyr), shorter-term variability is approximately in the 0.2–0.5‰ range. In addition to the longer-term increase in $\delta^{18}O$ values, we also observe three distinct time periods during which isotope values display heavier than average values: around ~26.5–26.9 Ma, 27.6–28.0 Ma, and 28.8–29.2 on our timescale (Figure 2). Each one of these periods of heavy isotope values consists of one or two individual events, separated by 100–200 kyr.

3.2. Benthic Foraminifera Carbon Isotopes

[8] The range of carbon isotope values obtained here is comparable to previous, lower-resolution measurements from the central equatorial Pacific (DSDP 77, 574). The median value of benthic $\delta^{13}C$ values is 0.45‰, with a standard deviation of 0.25‰. The total range of values spans −0.18 to 1.09‰. Similar to the oxygen isotope

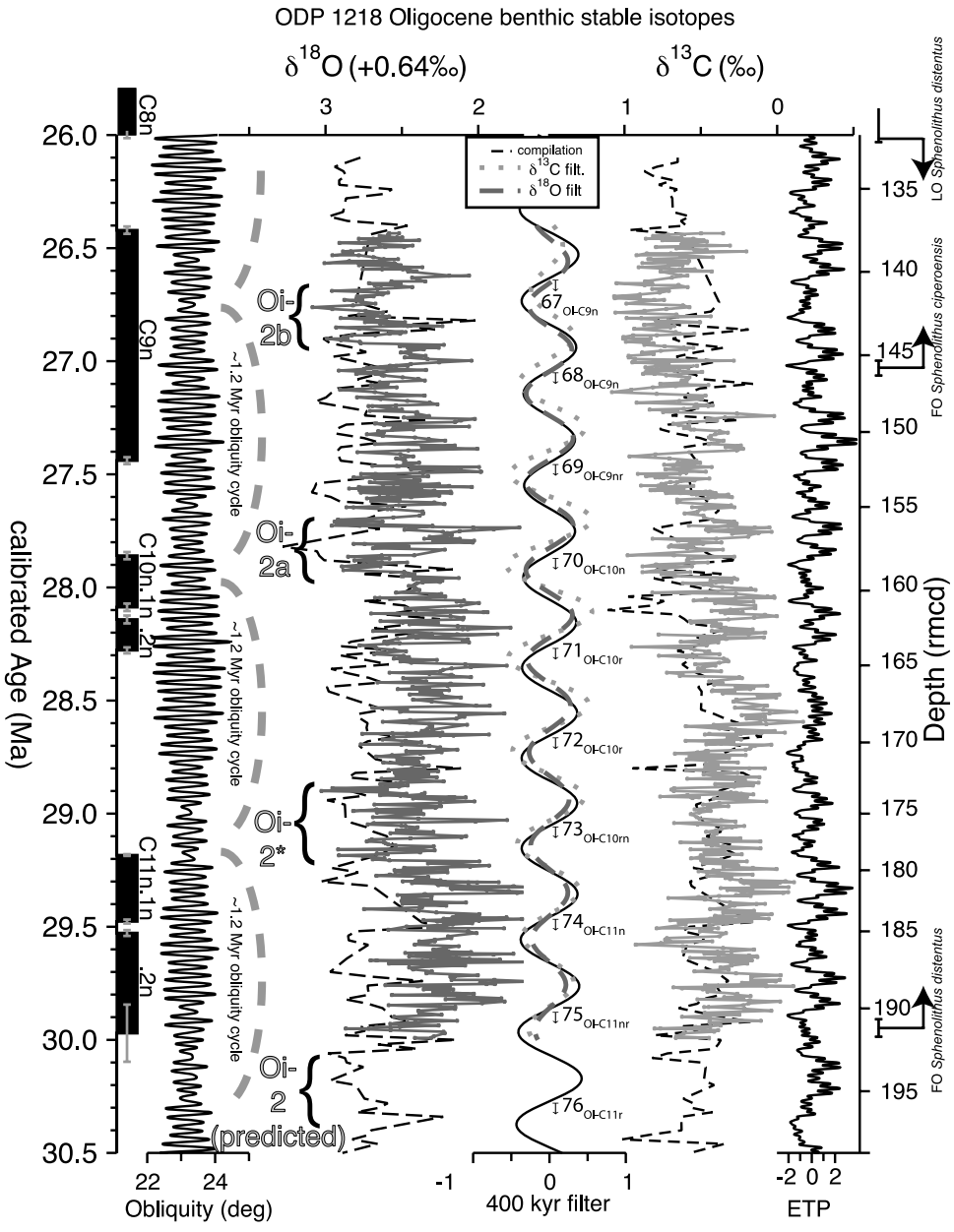

Figure 2. Benthic oxygen and carbon isotope measurements from Site 1218 plotted against astronomical age. Also shown are calculated obliquity and an "ETP" (eccentricity, tilt, and climatic precession) mix, derived from *Laskar et al.* [2004b]. Bandpass filters for eccentricity and stable isotope measurements were calculated for the ~405 kyr long eccentricity component, and are the basis for a new event naming scheme, as annotated. Compilation data are from *Zachos et al.* [2001b] and were age adjusted to our new timescale by mapping from the magnetostratigraphy of *Cande and Kent* [1995] to the magnetochrons determined for Site 1218 [*Shipboard Scientific Party*, 2002]. Shown for reference are selected nannofosssil datums observed at Site 1218. Brackets span intervals that correlate to previously observed glacial ("Oi") events. The position of Oi-2 is predicted on the basis of the astronomical pattern. See color version of this figure in the HTML.

values, the benthic $\delta^{13}C$ record also displays a trend toward heavier values from old to young; the linear component across the record yields ~0.47‰. The majority of this shift occurs above 165 rmcd, or younger than ~28.5 Ma (Figure 2). On <100 kyr timescales, the amplitude variation of $\delta^{13}C$ is in the 0.2–0.4‰ range, while larger variability in the ~0.5–1.0‰ range occurs on eccentricity timescales. Similar to previous studies [*Paul et al.*, 2000; *Zachos et al.*, 2001b], the benthic carbon isotope record shows a very strong response on a ~405 kyr timescale, as judged by an

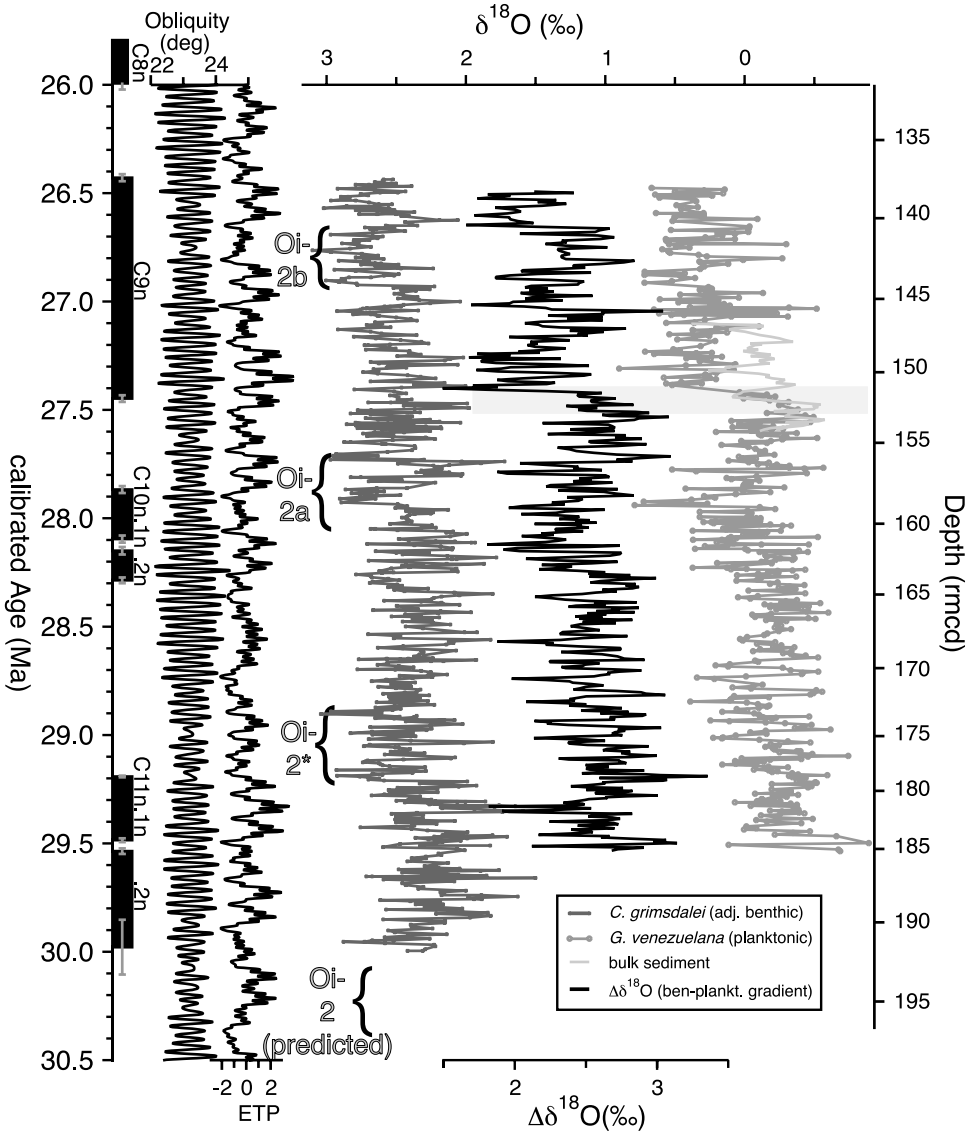

Figure 3. Benthic, planktonic, and bulk oxygen isotope measurements from Site 1218, as well as benthic-planktonic oxygen isotope gradient. Benthic isotope values are adjusted by adding 0.64‰. The shaded area marks an interval with a strong shift of planktonic isotope values that is not represented in the benthic foraminiferal record. See color version of this figure in the HTML.

initial match of the magnetostratigraphy to the timescale of *Cande and Kent* [1995].

3.3. Planktonic Foraminifera Oxygen Isotopes

[9] Planktonic foraminifera oxygen isotope values record high and low frequency variability and fluctuate between −0.88 and 0.91‰ (Figure 3). Toward the younger end of the record there is an increase in $\delta^{18}O$ values with a mean of −0.35‰ at 29.4 Ma, increasing to 0.30‰ at 26.5 Ma. Short frequency (<50 kyr) changes are generally minor (0.5‰), with higher-amplitude variations of 1.2‰ occurring on 80 to 120 kyr timescales. An enrichment in $\delta^{18}O$ is recorded at 28.4 Ma, where oxygen isotope values increase by 1.39‰ over 500 kyr from −0.59‰ at 28.44 Ma to 0.80‰ at 27.92 Ma. Planktonic foraminiferal oxygen isotope values then become lighter again to −0.48‰, before a short-term increase in $\delta^{18}O$ at 27.54 Ma, where oxygen isotope values change from −0.48‰ to 0.50‰ over 170 kyr. Increases in planktonic foraminiferal oxygen isotope values for 70 to 160 kyr are recorded at 29.16, 27.91 and 26.76 Ma. Oscillations in $\delta^{18}O$ (1‰) with a period of ∼110 kyr are particularly evident from 29.0 Ma to 28.5 Ma. The vertical oxygen isotope difference between planktonic and benthic foraminifera ($\Delta\delta^{18}O$) was calculated and is also shown in Figure 3. The gradient varies between 1.64 and 3.28‰. From 29.5 to 26.4 Ma mean $\Delta\delta^{18}O$ decreases slightly from 2.7‰ to 2.3‰.

3.4. Planktonic Carbon Isotope Results

[10] Pronounced, cyclic variations are recorded in the $\delta^{13}C$ values from *Globoquadrina venezuelana* of the Oligocene at Site 1218, between 0.32 and 1.67‰ (Figure 4).

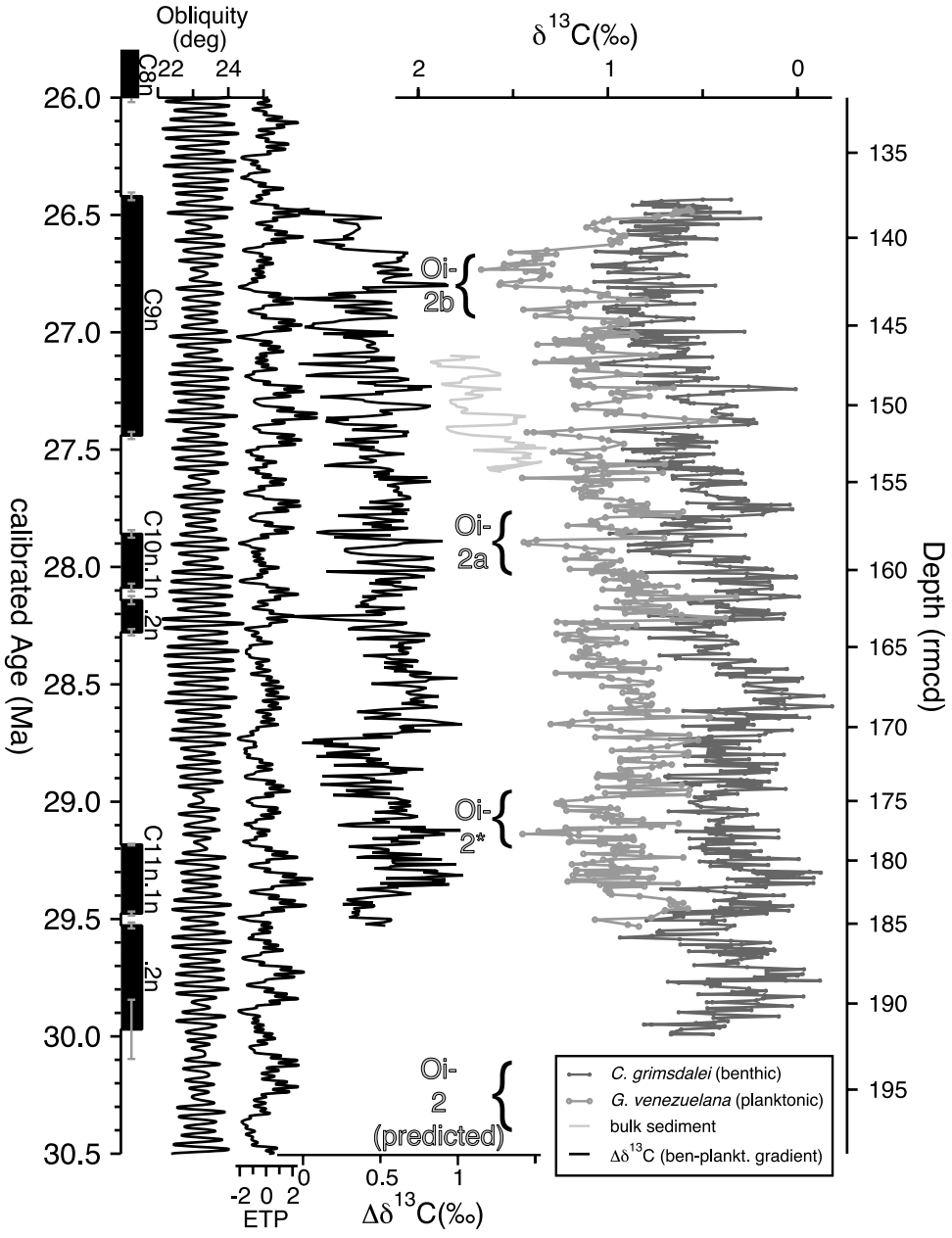

Figure 4. Benthic, planktonic and bulk carbon isotope measurements from Site 1218, as well as benthic-planktonic carbon gradient. See color version of this figure in the HTML.

Variations in $\delta^{13}C$ are recorded in 405 and 100 kyr eccentricity cycles, which are particularly apparent toward the upper part of the record. Maxima in planktonic foraminifera carbon isotopes (1.5‰) are recorded on 1.2 Myr timescales at 29.16, 27.91 and 26.76 Ma. In general, trends in the planktonic foraminifera $\delta^{13}C$ record match those from the benthic foraminiferal $\delta^{13}C$ record, but with a higher degree of variability.

[11] The difference of $\delta^{13}C$ between planktonic *G. venezuelana* and benthic *C. grimsdalei* is small (Figure 4), and ranges from a minimum of 0‰ to a maximum of 1‰. The increased gradient in $\delta^{13}C$ reoccurs on a 405 kyr cycle, and is mainly due to enrichment of $\delta^{13}C$ in planktonic foraminifera.

3.5. Stable Isotope Measurements From Bulk/Fine Fraction Samples

[12] Fine fraction bulk analyses reveal changes in $\delta^{18}O$ between −0.56 and 0.39‰ (Figure 3). Although the record of bulk carbonate is short (526 kyr), the $\delta^{18}O$ signal is cyclic at the short-term (∼100 kyr) eccentricity period. The bulk $\delta^{18}O$ measurements are distinctly lighter than planktonic foraminiferal values, particularly between 27.39 and 27.12 Ma, yet also record an

increase of $\delta^{18}O$ values toward the younger end of the interval measured.

[13] High-amplitude, cyclic changes are recorded in the fine fraction bulk $\delta^{13}C$ data, between 1.33 and 1.94‰ (Figure 4). The $\delta^{13}C$ bulk values are generally 0.7‰ heavier than those recorded by the planktonic foraminifera *G. venezuelana*, but also show cyclic shifts on the short eccentricity scale (~100 kyr). Amplitude variations of individual cycles are strongly coherent with those of the planktonic record. Similar to the bulk $\delta^{18}O$ measurements, the bulk $\delta^{13}C$ values also increase toward the younger end of the measured interval. An interesting feature is the smoothness of the bulk $\delta^{13}C$ record for timescales shorter than eccentricity. All stable isotopic data from foraminifera and bulk carbonate measurements are tabulated in a data report [*Wade and Pälike*, 2004].

3.6. Timescale Generation

[14] ODP Site 1218 provided a high-resolution (~1–2 cm/kyr) biogenic sediment record from the late Paleocene to the early Miocene. These sediments were found to contain an uninterrupted set of geomagnetic chrons, as well as a detailed record of calcareous and siliceous biostratigraphic datum points [*Shipboard Scientific Party*, 2002]. Shipboard lithological proxy measurements and shore-based X-ray fluorescence scanning revealed clearly recognizable cycles that can be attributed to climatic change, driven by Milankovitch style orbital variations of the Earth. Discovering drill sites with a well-defined magnetostratigraphic and biostratigraphic record that also show clear lithological cycles is rare and valuable, and opened the opportunity to develop a detailed stratigraphic intersite correlation (H. Pälike et al., Integrated stratigraphic correlation and improved composite depth scales for ODP Sites 1218 and 1219, submitted to *Ocean Drilling Program Scientific Results*, 2004), as well as providing the data to refine and extend the astronomical age calibration for the Oligocene. Lithological proxy parameters that were obtained from depth-adjusted and stacked records from ODP Sites 1218 and 1219, XRF elemental concentration measurements and stable isotope measurements were used to refine our astronomical timescale.

[15] Carbonate content (%$CaCO_3$), estimated from XRF and MST data, varies from 80 to 93% during the studied interval. Both, oxygen and carbon fine fraction measurements, also correlate very highly with lithological indicators of $CaCO_3$ content. These records show an exceptionally strong imprint of both short (~110 kyr) and long (~405 kyr) eccentricity, in addition to a weaker imprint of both obliquity (~40 kyr) and climatic precession (~21 kyr). The imprint of several amplitude modulations in the astronomically driven lithological and stable isotope records provide a strong relative age control. The basis for our age model was a new astronomical calculation [*Laskar et al.*, 2004a, 2004b], that was also used in the timescale generation. An additional study [*Pälike et al.*, 2004] showed that this new astronomical solution provides a better fit with geological data than previous solutions, at least back to ~30 Ma.

[16] Our data show a much stronger relative spectral power at both eccentricity periods (~100 and ~405 kyr) than insolation calculations. Thus we created an artificial "ETP" (eccentricity, tilt, precession) mix with an enhanced eccentricity component to make our data visually more comparable with the target curve. The age model is primarily based on the eccentricity signal in the data, and was constructed such that light stable isotope values correspond to eccentricity maxima, consistent with previous studies [*Shackleton et al.*, 1999a; *Zachos et al.*, 2001b], and guided by obliquity amplitude modulation patterns.

4. Discussion

[17] The orbitally adjusted timescale and detailed stable isotope data set for both planktonic and benthic foraminifera for Site 1218 provide a comprehensive analysis of Oligocene oceanographic development, particularly in regards to temperature, paleoproductivity and the evolution of the early Cenozoic cryosphere.

4.1. Comparison With Previous Deep-Sea Records

[18] In Figure 2, the benthic isotope results are plotted with previous results from ODP and DSDP sites (data compiled by *Zachos et al.* [2001a], adjusted to our timescale). Benthic foraminifera carbon isotope results are consistent with previous records from both Atlantic, Pacific and Southern Ocean sites. The close correspondence in $\delta^{13}C$ values recorded at a number of sites from different oceans and different latitudes indicates that the Oligocene oceans were homogeneous and the $\delta^{13}C$ gradient between the oceanic basins was absent or small during the Oligocene, and was also observed by *Billups et al.* [2002]. The $\delta^{13}C$ variations, on at least eccentricity frequencies or lower, are thus reflecting a global signal rather than a regional record.

[19] The $\delta^{18}O$ results of benthic foraminifera at Site 1218 are comparable in value to data elsewhere, except ODP Sites 689, 690 and 748 in the compilation of *Zachos et al.* [2001a], which are generally 0.3‰ heavier, indicative of cooler and/or more saline deep water around Antarctica.

4.2. Paleoecology of *Globoquadrina Venezuelana*

[20] The paleobiology of Oligocene planktonic foraminifera is poorly constrained. Information on the depth habitat of extinct planktonic foraminifera can be attained through multispecies stable isotope analyses (see *Pearson et al.* [1993] for discussion). While it is now established which species occupied the mixed layer through much of the Cenozoic, very few studies have been performed on Oligocene planktonic foraminifera. Groups such as paragloborotaliids have been documented as surface [*van Eijden and Ganssen*, 1995], thermocline (B. Wade, unpublished data, 2004) and subthermocline dwellers [*Douglas and Savin*, 1978]. The same problem exists for *Globoquadrina venezuelana*, where oxygen isotope values suggest an intermediate dwelling by *Biolzi* [1983], but is documented as deep dwelling form in the Miocene [*Gasperi and Kennett*, 1993]. Multispecies analysis (B. Wade, unpublished data, 2004) and comparison with bulk isotope data suggest that *G. venezuelana* was an upper thermocline dweller. The resulting isotope analyses are thus not considered to reflect those of the mixed layer and are

probably heavier in $\delta^{18}O$ and lighter in $\delta^{13}C$ than those of surface dwelling planktonic foraminifera.

[21] We observe a clear step (1.39‰) in the oxygen isotope values of *G. venezuelana* at 27.4 Ma (Figure 3). However, this change is not associated with any of the Oi events and is not reflected in the benthic foraminiferal record, suggesting that the heavy $\delta^{18}O$ in planktonic foraminifera are not related to a major increase in ice volume. Bulk oxygen isotope results show a general decrease in $\delta^{18}O$ but do not match the oxygen isotope record of *G. venezuelana*. Comparison with the percent carbonate, color and physical properties values over this interval also reveal no comparable alteration. Unlike the Oi events the increased $\delta^{18}O$ values are associated with a decrease in $\delta^{13}C$ from 1.4 to 0.5‰. The nature of this event is therefore different to the forcing mechanisms elsewhere in the record. This shift may reflect changes in surface water circulation related to flow through the Central American gateways or a slightly cooler water mass as the site moves north of the equator. Alternatively the decrease in both $\delta^{18}O$ and $\delta^{13}C$ may indicate a change in the depth habitat of *G. venezuelana* from the upper thermocline, as suggested by multispecies data (Wade, unpublished data, 2004) to a deeper dwelling form, similar to the Miocene [*Gasperi and Kennett*, 1993].

4.3. Diagenesis and Isotope Fractionation Effects in Deep-Sea Carbonate

[22] Recrystallization of foraminiferal specimens is evident in the scanning electron microscope (SEM) images of planktonic foraminifera at Site 1218 (Figure 1). The SEM images (of unsonicated specimens) reveal partial recrystallization of test walls, attached secondary calcite, and some infilling of pores and apertures. Specimens chosen for isotopic analysis were devoid of calcite infilling and sonication was applied to remove attached calcite.

[23] Carbonate diagenetic processes are likely to have altered the primary $\delta^{18}O$ signal and increased the oxygen isotope values of planktonic foraminifera [*Schrag et al.*, 1992, 1995]. This may cause paleotemperatures reconstructed from tropical planktonic foraminifera to be underestimated [*Pearson et al.*, 2001]. There is no means of constraining this diagenetic offset at present, but it nevertheless must be small relative to the signal amplitude. The preservation of distinctive stable isotope signals, particularly in the carbon isotope record, the cyclic nature of the data, and the large (2.5‰) gradient in $\delta^{18}O$ between *G. venezuelana* and benthic foraminifera isotope values suggests that diagenesis did not destroy the original signal. Additional multispecies analysis (not shown) reveals clear offsets in $\delta^{18}O$ between species, which are not expected to be retained if the tests were completely recrystallized.

[24] To assess the preservation of carbonate, nannofossil assemblages were examined from intervals of both high and low $\%CaCO_3$ and $\delta^{13}C$. These showed no obvious preservational differences (J. Backman and I. Raffi, personal communication, 2004), suggesting that the changes in $\delta^{13}C$ are not of secondary, diagenetic origin. Samples were dominated by the nannofossil *Cyclicargolithus floridanus*, however, one key component of the assemblages in high carbonate and heavy $\delta^{13}C$ intervals were the increased size of nannoplankton and the abundance of sphenoliths. Sphenoliths were previously documented as k-selected species, being adapted to a warm water, oligotrophic and stable environment [*Haq and Lohmann*, 1976; *Haq*, 1980; *Lohmann and Carlson*, 1981; *Perch-Nielsen*, 1985; *Aubry*, 1992]. However, their paleoecology has recently been questioned by *Gibbs et al.* [2004] who noted a covariance between the abundance of sphenoliths and productivity variations during the Pliocene. B. Wade and P. Bown (Calcareous nannofossils in extreme environments: The Messinian salinity event, submitted to *Palaeogeography, Palaeoclimatology, Palaeoecology*, 2004) also noted a high abundance and almost monospecific assemblages of sphenoliths in diatom rich samples from the Messinian, Cyprus. This would suggest that contrary to previous reports, sphenoliths were capable of inhabiting a wide range of environments, and enhanced their abundance during high productivity intervals. This finding is particularly important as it suggests the shifts in planktonic foraminiferal and bulk isotope $\delta^{13}C$ are a direct response to productivity changes in surface waters, and not a secondary effect of diagenetic alteration. The corresponding cyclic changes in percent carbonate and increases in $\delta^{13}C$ suggest an enhanced production of biogenic material and equatorial Pacific productivity fluxes that were directly related to oscillations in solar insolation.

4.4. Orbital Climate Forcing During the Oligocene

[25] The recognition of isotope variability that might be associated with orbital climate forcing relies on high-resolution records from the same site. Even though moderate-resolution records exist for the Oligocene as part of data compilations [*Zachos et al.*, 2001a], stratigraphic correlation uncertainties, different depositional settings, water depths and latitudes between sites that are part of these compilations make the identification of orbitally influenced variability difficult.

[26] The high-resolution isotope records from Site 1218 have enabled us to document the effect of orbital forcing on the Oligocene climate. In order to evaluate the relative strength of potential astronomical forcing in the stable isotope data of this study, and to estimate phase relationships between the time series, we performed cross-spectral analyses between the benthic and planktonic $\delta^{18}O$ and $\delta^{13}C$ measurements that were presented in Figures 2, 3 and 4. These spectra, coherency estimates and phase plots are shown in Figure 5.

[27] The confidence intervals in Figure 5 solely depend on the sample spacing, and the spectral analysis method used, and do not depend on the choice of a particular noise model. The interpretive choice of a noise null-model determines to what level of significance spectral peaks cannot be explained by noise. Paleoclimatological data often exhibit a red-noise pattern, with higher power at lower frequencies, and autoregressive models are used to calculate a best fitting noise continuum. We provide auxiliary material that demonstrates the significance estimates for benthic $\delta^{13}C$ spectral peaks by assuming a red-noise background. However, statistical tests [*Schulz and Mudelsee*, 2002] performed on

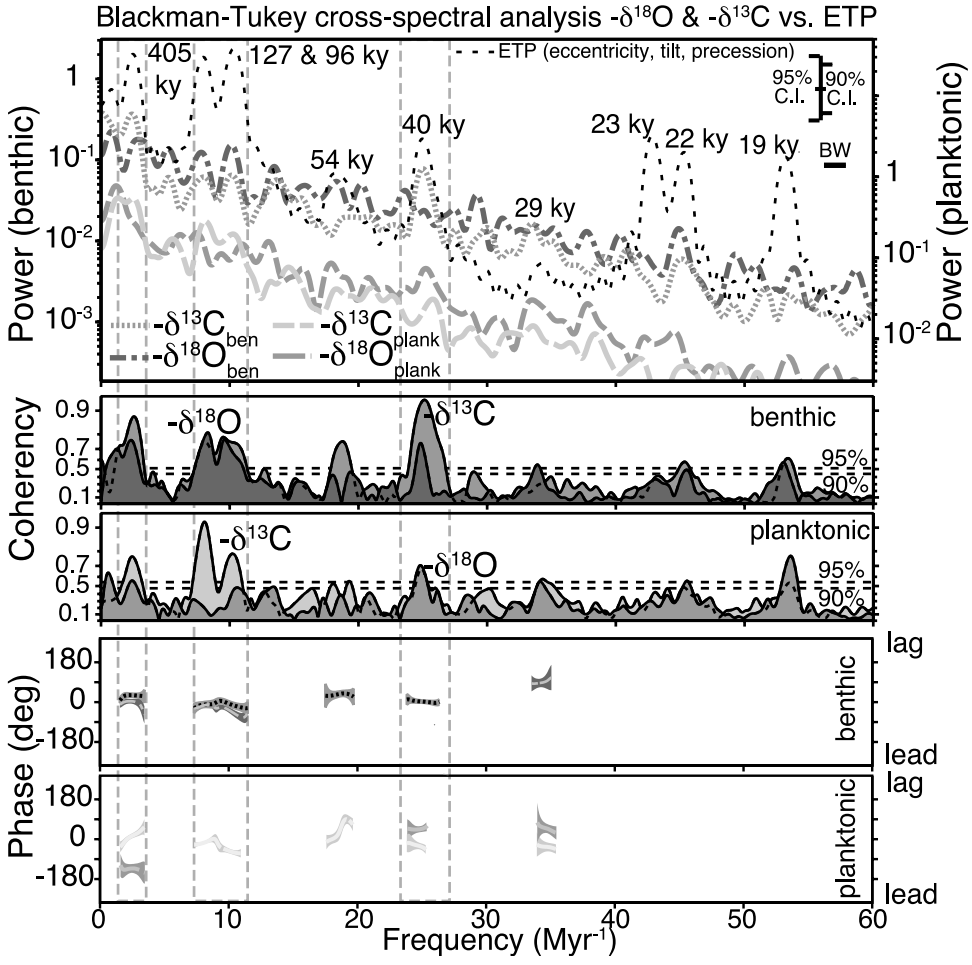

Figure 5. Blackman-Tukey cross-spectral analysis of benthic and planktonic stable isotopes, against astronomical tuning target ETP. Both astronomical and stable isotope series were re-sampled at equal intervals corresponding to the median time step of ~6 kyr. Cross-spectra, confidence intervals (C.I.), and bandwidths (BW) were calculated with 140 lags after linear detrending. Phase estimates are plotted only where coherency values are significant and spectral power is present. The eccentricity and obliquity frequency bands are marked by bars. Stable isotope values were flipped prior to analysis. Spectra were calculated with AnalySeries [*Paillard et al.*, 1996]. See color version of this figure in the HTML.

our spectra reveal that a red-noise model is not appropriate to describe the spectra, which do not show the indicative straight-line shape on log-log frequency versus spectral power plots. Instead, our noise-spectra are best matched with an exponential fit (supplementary material).

[28] In our data, spectral power is strong with significant coherence for the 40 kyr obliquity band in the benthic $\delta^{13}C$ data. Benthic isotope data and planktonic $\delta^{13}C$ all show a strong response around the short (~100 kyr) eccentricity cycle, and all four stable isotope series show strong peaks with significant coherence in the long eccentricity (~405 kyr) band. It is possible that an even higher sample resolution might increase the spectral power in the climatic precession band (~19–23 kyr).

[29] Power in the orbital bands of eccentricity (406, 130–94 kyr) and obliquity (40 kyr) is indicated by spectral analysis of the isotopic records. Cross-spectral analysis reveals significant coherency between the stable isotope records and orbital forcing and indicates that the Oligocene climate was sensitive to orbital changes in solar insolation.

[30] The benthic stable isotope time series show a strong and coherent response at the ~100 and ~405 kyr short and long eccentricity periods. This eccentricity imprint is also reflected in the planktonic isotope series, but with a less clear response to short eccentricity in the planktonic $\delta^{18}O$ series. The pronounced ~100 and ~405 kyr periodicity within the isotope records confirms the importance of eccentricity oscillations in pre-Pleistocene climate.

[31] Surprisingly, the benthic carbon isotope record shows a stronger response at the ~40 kyr obliquity period than the benthic oxygen isotope record, for which the obliquity peak is offset toward slightly lower frequencies, and for which filters display a less stable phase relationship, thus reducing its power. Phase estimates are only meaningful where spectral power (and coherency) values are high.

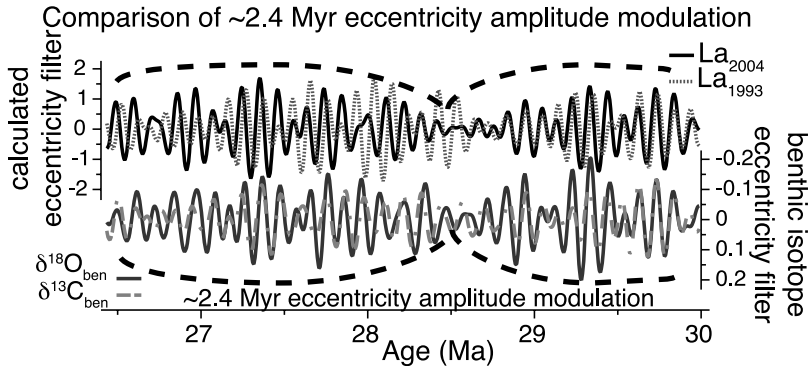

Figure 6. Comparison of ~2.4 Myr eccentricity modulation of the short ~100 kyr eccentricity cycle of two astronomical models [*Laskar et al.*, 1993, 2004b] and benthic stable isotope time series. See color version of this figure in the HTML.

[32] The phase relationships at the eccentricity periods are as expected for the benthic stable isotopes, but the response of planktonic $\delta^{18}O$ is 180 degrees out of phase with the other three isotope records. The individual short eccentricity cycles are not completely symmetric, thus some difference in phases can be expected. A lag of planktonic oxygen isotopes with respect to the planktonic carbon record at the obliquity frequency is also suggested. We cannot make any confident predictions about phase relationships at the climatic precession frequencies yet, but anticipate that an increased sample resolution could enhance our observations.

[33] The short eccentricity cycle, present in lithological as well as stable isotope data, is amplitude modulated with a period of ~2.4 Myr. This amplitude modulation pattern is consistent with that of astronomical target curves (Figure 6), and together with the clear ~405 kyr eccentricity cycles (Figures 2 and 5) supports our age model.

[34] High-resolution studies from the late Oligocene/early Miocene have shown a pervasive imprint of orbital frequencies in various climate proxies and stable isotope measurements [*Shackleton et al.*, 1999a, 2000; *Paul et al.*, 2000; *Zachos et al.*, 2001b; *Billups et al.*, 2002, 2004]. These studies, from both high and low latitude sites, have demonstrated several characteristic features of orbital forcing in the Oligocene climate. In particular, a strong imprint of the ~405 kyr long eccentricity cycle has been found to be consistently associated with dominant variations of $\delta^{13}C$ records. During the Oligocene, these long eccentricity cycles, as recorded in the isotope records, appear to be synchronized in phase for records from different latitudes [*Billups et al.*, 2004], and without any significant ocean-to-ocean gradient, at least during the late Oligocene and early Miocene [*Billups et al.*, 2002]. In addition, the ~405 kyr long eccentricity cycle is also being considered as the most stable of the Earth's long-term astronomical frequencies [*Laskar*, 1999].

[35] Owing to its global nature, matching long eccentricity cycles with those found in stable isotope measurements provides an ideal cyclostratigraphic correlation tool. What makes the long eccentricity cycle imprint particularly interesting is the suggestion that geological records on this timescale could potentially also show a relationship with eustatic sea level change and sequence boundaries [*Gale et al.*, 2002; *Hardenbol*, 2003].

4.5. Obliquity Nodes and Glacial Forcing

[36] Previous studies from the Pliocene/Pleistocene implicated periods of obliquity maxima, modulated with a period of ~1.2 Myr, with times of enhanced glaciations [*Lourens and Hilgen*, 1997]. In addition to the ~100 and ~405 kyr short and long eccentricity cycles demonstrated in Oligocene data sets, we also find a strong direct imprint of the ~1.2 Myr obliquity cycle (Figure 2). In astronomical calculations, this cycle is present mainly through its amplitude modulation of the ~40 kyr obliquity cycle.

[37] In contrast to the Pliocene/Pleistocene, studies from the Miocene and Oligocene [*Zachos et al.*, 2001b; *Turco et al.*, 2001] found the opposite: periods of low obliquity amplitude variations correspond to glacial events and periods. Our data confirm this view: we find a ~1.2 Myr amplitude modulation of the recorded obliquity signal in the benthic $\delta^{13}C$ data. We also find a direct imprint of the 1.2 Myr cycle in our benthic oxygen isotope data, where intervals with particularly heavy isotopes correspond to minima of the 1.2 Myr obliquity amplitude cycle, and generally to minima in the ~405 and ~100 kyr eccentricity cycles. The direct imprint of the 1.2 Myr cycle most likely arises through an enhanced sensitivity of the cryosphere to low variations in seasonality. *Zachos et al.* [2001b] suggested that it is the prolonged absence of particularly warm (Southern Hemisphere) summers rather than the occurrence of particularly cool ones that is the significant astronomical factor for inhibiting summer ice melt and thus triggering ice sheet initiation. On the basis of our data, we can support this hypothesis, and postulate that glaciations during the Oligocene are primarily driven by the eccentricity cycles, but with enhanced probability of glaciations during intervals of low obliquity amplitude variations. The 1.2 Myr glacial cycles suggest that ice sheets on Antarctica were dynamic and sensitive to orbital variations of solar insolation. This pattern is also observed in additional studies from Site 1218 for lower parts of the Oligocene [*Coxall et al.*, 2004] which suggests that this relationship between obliquity minima and glaciations has been consistent for at

Table 1. Isotope Events Summary

			Biozones		Maximum, ‰		Amplitude, ‰				
Code/Chron	δ^{18}O Event	Age, Ma	Foram	Nanno	$\delta^{18}O_{ben}$	$\delta^{18}O_{pl}$	$\delta^{18}O_{ben}$%	$\delta^{18}O_{pl}$	Duration, kyr	Ice Volume, ‰[a]	Eustatic Change, m[b]
$67_{Ol\text{-}C9n}$	Oi-2b	26.76	P21b	CP19b	3.00	0.73	0.86	0.85	160–236	0.65	59
$70_{Ol\text{-}C10n}$	Oi-2a	27.91	P21b	CP19a	2.90	0.80	0.77	1.01	70–130	0.58	53
$73_{Ol\text{-}C10rn}$	Oi-2*	29.16	P21a	CP19a	2.92	0.17	0.93	0.75	106–136	0.70	64
$76_{Ol\text{-}C11r}$	Oi-2	30.35	P20	CP18							

[a]Here 75% of δ^{18}O benthic foraminiferal increase attributed to ice volume [*Fairbanks*, 1989].
[b]Here 0.11‰ increase in δ^{18}O/10 m sea level fall [*Fairbanks and Matthews*, 1978].

least 15 Myr between the earliest Oligocene and the Miocene.

4.6. A new Paleogene Cyclostratigraphic Naming Scheme, in Relation to Glacial Isotope Events

[38] Previous studies designated named glaciation "events" in the Paleogene, based on intervals where particularly heavy oxygen isotope ratios were observed from several sites, interpreted to represent global changes in ice volume [*Miller et al.*, 1991; *Pekar and Miller*, 1996; *Zachos et al.*, 1996; *Pekar et al.*, 2002]. In general, these events were numbered consecutively from old to young for each epoch ("Oi-x" for the Oligocene, "Mi-x" for the Miocene etc., where x represents a number/letter code).

[39] Several problems exist with these naming schemes. First, different authors designated the same event name to different events: Oi-1a and Oi-1b are defined differently in the work of *Miller et al.* [1991] and *Zachos et al.* [1996], respectively. Second, the named events were based on relatively low-resolution records from a limited number of sites. Thus as more and higher-resolution records became available, a larger number of heavy oxygen isotope ratio time intervals were recognized, not only resulting in the augmentation of existing event names by additional letter codes, but also additional "unnamed" events [*Pekar and Miller*, 1996]. Third, higher-resolution records, as the one presented in this study, show that some of the previously defined glaciation events in the Oligocene instead comprise several oxygen isotope maxima, implying that the previous lower-resolution records can result in the correlation of separate events that were close, but not identical. Finally, the lack of detailed additional magnetostratigraphic control meant that it was not always obvious where these events were correctly placed stratigraphically. For these reasons, we propose here a new naming scheme that relates astronomical (chronological) information with magnetostratigraphy, in order to provide a more consistent framework for identifying and correlating global isotope events during the Paleogene.

[40] The original studies that defined and correlated the "Oi-x" glaciation events [*Miller et al.*, 1991; *Pekar and Miller*, 1996; *Miller et al.*, 1998] linked these to glacio-eustatic sea level changes as observed from seismic sequence stratigraphy. Additional studies suggested that third-order sequences might be intricately related to ~405 kyr eccentricity cycles [*Gale et al.*, 2002; *Hardenbol*, 2003]. In our records, as well as other records from the late Oligocene/early Miocene [*Paul et al.*, 2000; *Zachos et al.*, 2001b; *Billups et al.*, 2004], the ~405 kyr eccentricity cycle is very well expressed in stable isotope records, particularly in δ^{13}C records. As this frequency component of Earth's eccentricity cycle is considered relatively stable over geological time [*Laskar*, 1999], it has been proposed previously as the basis for chronostratigraphic correlation and timescale designations [*Shackleton et al.*, 1999b].

[41] For different astronomical calculations [*Laskar et al.*, 1993, 2004b] individual ~405 kyr cycle ages differ by less than 200 kyr throughout the Cenozoic, thus a cycle count number for a given absolute age is unique to within one cycle. Our new scheme is to define events by 405 kyr cycle numbers as follows. The cycle count number is defined by ~405 kyr eccentricity minima from *Laskar et al.* [2004b]. Cycle count numbers increase going back in time, starting with count number 1 for the cycle comprising the most recent minimum, ~10 kyr before present. We define each cycle number to end at the younger zero crossing following each ~405 kyr eccentricity minimum. In addition to the cycle count, which is a formal part of our designation, we extend this code for practical purposes to also include a subscripted code for the geological epoch together with the magnetochron closest to the ~405 kyr eccentricity minimum (following the style of *Cande and Kent* [1995], but excluding subchrons, e.g., C6n instead of C6Cn.1n, and appending rn or nr where the cycle falls close to a reversal). This coding scheme is illustrated in Figure 2. We propose that one could extend this scheme to include ~100 kyr eccentricity cycles (and maybe also shorter obliquity/climatic precession cycles) within the ~405kyr eccentricity cycle framework.

4.7. "Oi" Stable Isotope Events

[42] Previous Oligocene glacial events have been defined and described by *Shackleton* [1986], *Miller et al.* [1987, 1991], *Wright et al.* [1992], *Pekar and Miller* [1996], and *Pekar et al.* [2002]. Sequence stratigraphic studies and continental margin sequences of the Oligocene [*Browning et al.*, 1996; *Miller et al.*, 1996; *Pekar et al.*, 2000; *Kominz and Pekar*, 2001] correspond to a number of notable enrichments (>0.5‰) in Oligocene benthic foraminiferal δ^{18}O records [*Pekar et al.*, 2002]. These intervals have been interpreted as significant increases in Antarctic ice volume and support the oscillation of ice volume and sea level throughout the Oligocene *Miller et al.* [1987, 1991, 1998]; *Pekar and Miller* [1996]; *Pekar et al.* [2000, 2001].

[43] The lower resolution in previous studies has prevented the timing and magnitude of glacial (Oi) events being accurately defined. In our records, increases in δ^{18}O are evident in both the planktonic (0.75 to 1.01‰) and benthic (0.77 to 0.93‰) record at 29.16, 27.91 and 26.76 Ma (Figure 3). We interpret these events to correspond to the

Oi-2b (here assigned eccentricity cycle 67_{Ol}), Oi-2a (70_{Ol}) and Oi "unnamed" or Oi-2* (73_{Ol}), as defined by *Miller et al.* [1991] and *Pekar and Miller* [1996], but also recognize additional events close in time. The timing, amplitudes and durations of the various Oi events at Site 1218 are summarized in Table 1. Events are typified by covarying enrichment in planktonic and benthic $\delta^{18}O$ values (>0.7‰), heavy adjusted benthic oxygen isotope values (>2.9‰), and durations from ~70 to 240 kyr.

[44] The coeval shifts in benthic and planktonic $\delta^{18}O$ records are thought to indicate expansion in Antarctic ice volume. The amplitude of $\delta^{18}O$ variations at the Oi events within the planktonic foraminifera record is 0.75 to 1.00‰ and exceeds the magnitude recorded at Site 77 [*Keigwin and Keller*, 1984]. The interval of heavy oxygen isotope events are longer in the benthic foraminifera record than in the planktonic foraminifera record by approximately 30–70 kyr. This reflects substantial high-latitude cooling that preceded the ice volume increases, which are picked up by the benthic foraminiferal but not tropical planktonic foraminiferal record. The amplitude of $\delta^{18}O$ change in benthic foraminifera at Oi-2b (67_{Ol}) and Oi-2a (70_{Ol}) are comparable to those recorded at sites elsewhere [*Pekar et al.*, 2002]. However, we record a much greater change in benthic and planktonic $\delta^{18}O$ at Oi-2* (73_{Ol}) than in earlier studies. This arises because the event has previously been unresolved in low-resolution studies of the Oligocene. The covariance between planktonic and benthic foraminiferal oxygen isotope records indicates fluctuations in global ice volume and the sustained existence of oscillating ice sheets on Antarctica during the Oligocene.

[45] Increases in benthic foraminiferal $\delta^{18}O$ are also evident at intervals throughout the record (at 28.89, 28.27, 27.71 and 26.53 Ma). These episodes are 45 to 78 kyr in duration and are characterized by shifts in benthic $\delta^{18}O$ of 0.44 to 1.24‰ and heavy benthic oxygen isotope values (>2.90‰). They are associated with minor increases in planktonic foraminiferal $\delta^{18}O$ and are thought to reflect small changes in Southern Hemisphere ice volume. For lower-resolution studies there is therefore the potential to misidentify the Oi events for these shifts in benthic $\delta^{18}O$. While the original studies defined the Oi events based entirely on $\delta^{18}O$ values, the placement of the Oi events here is constrained through simultaneous increases in planktonic foraminiferal $\delta^{18}O$ and maxima in benthic and planktonic foraminiferal $\delta^{13}C$.

4.8. Ice-Volume Changes During the Oligocene

[46] Fluctuations in global ice volume, eustatic sea level, and temperature change during glaciation events can be constrained by comparing the amplitude of $\delta^{18}O$ variation between planktonic and benthic foraminifera. Oxygen isotope increases range from 0.77 to 0.93‰ and 0.75 to 1.01‰ in the benthic and planktonic foraminiferal records, respectively. While the amplitude of change in benthic foraminiferal $\delta^{18}O$ is 0.93‰ at Oi-2* (73_{Ol}), ice volume fluctuations cannot exceed the variation recorded in planktonic foraminifera $\delta^{18}O$ (0.75‰), the rest of change has to be attributable to deep sea temperature changes and/or salinity variations and other factors. If a maximum of 75% of the benthic foraminiferal increases are ascribed to ice volume [*Fairbanks*, 1989], this would suggest a glacial effect of 0.58 to 0.70‰ during the Oi events. The magnitude of change recorded at Site 1218 suggests there were large variations in the amount of ice on Antarctica during the Oligocene.

4.9. Eustatic Sea Level Change in Relation to Oi Events

[47] Previous workers have suggested that third-order eustatic sea level changes, identified from seismic reflection profiles, are related to orbitally influenced climate variations, particularly the ~405 kyr eccentricity cycle [*Gale et al.*, 2002; *Hardenbol*, 2003] but also the ~1.2 Myr obliquity amplitude modulation cycle [*Lourens and Hilgen*, 1997].

[48] On the basis of a the late Pleistocene calibration of 0.11‰ increase in $\delta^{18}O$ per 10 m sea level fall [*Fairbanks and Matthews*, 1978], the eustatic fall at the Oi events is of the order of 50 to 65 m (Table 1). This is comparable with the eustatic change estimated by *Pekar and Miller* [1996] of 45 to 75 m during Oi-2b (67_{Ol}), but has been further constrained here by the planktonic foraminiferal $\delta^{18}O$ record. Using simultaneous changes between benthic and planktonic oxygen isotope values as an indicator of eustatic sea level changes, we calculated a relative sea level curve by multichannel singular spectral analysis with the software SSA Toolkit [*Ghil et al.*, 2002]. We selected those spectral components that are common to both signals, and reconstructed a combined smoothed time series (Figure 7). Our records indicate that one can match third-order eustatic sea level variations with high resolution oxygen isotope records, and that major glaciation cycles are indeed driven by the confluence of eccentricity cycles and longer-term obliquity amplitude variations.

4.10. Paleotemperature Estimates From Stable Isotope Measurements

[49] Several factors need to be taken into consideration in the calculation of paleotemperatures from foraminifera. This includes the ambient isotopic composition of seawater ($\delta^{18}O_{sw}$) in which the foraminiferal calcite was precipitated (which is influenced by salinity and global ice volume), diagenetic modification [*Schrag et al.*, 1992, 1995; *Pearson et al.*, 2001], and the concentration of seawater carbonate ion [*Spero et al.*, 1997; *Zeebe et al.*, 1999; *Russell and Spero*, 2000]. These limitations have to be considered in the following discussion, and we regard paleotemperatures to be estimated values and not absolute. Owing to the uncertainty regarding diagenetic imprint of $\delta^{18}O$, salinity of the Oligocene tropical ocean and the unconstrained depth habitat of *G. venezuelana* it was not possible to calculate sea surface temperatures for the Oligocene tropical Pacific. Paleotemperatures were calculated from adjusted benthic foraminiferal oxygen isotope measurements assuming constant ice volume and salinity. While we recognize that uniform ice volume is not correct this equation provides a gauge of general variation in deep sea temperatures.

[50] Our adjusted benthic oxygen isotope values vary around a median value of ~2.4‰. At this time Antarctica was partially glaciated. Additional measurements of Mg/Ca ratios from the same interval and the same site [*Lear et al.*, 2004] indicate that the average bottom water temperature

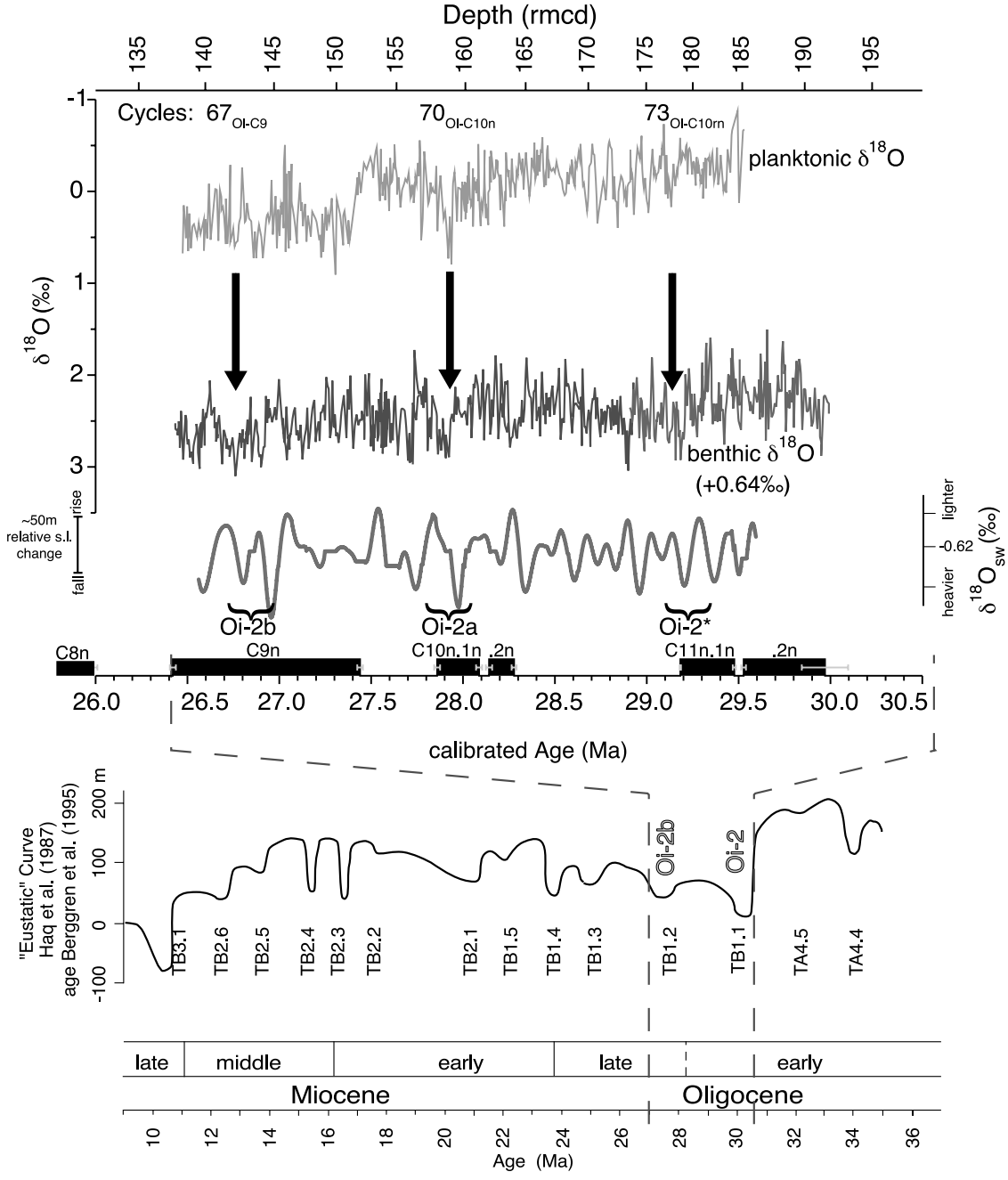

Figure 7. Sea level variation estimates based on covariation of benthic and planktonic oxygen isotope measurements and in relation to sequence stratigraphic estimates of sea level variations. The eustatic sea level curve of *Haq et al.* [1987] was age adjusted to the timescale of *Cande and Kent* [1995]. A comparison of the median benthic $\delta^{18}O$ values and derived temperature estimates [*Erez and Luz*, 1983] with Mg/Ca temperatures estimates from the same site [*Lear et al.*, 2004] results in a seawater oxygen isotope ratio of approximately −0.62‰ compared to present. See color version of this figure in the HTML.

for the time interval studied here was 3.6 ± 1.0°C, assuming modern seawater Mg/Ca. Combining this estimate with the equation of *Erez and Luz* [1983] results in an average $\delta^{18}O_{sw}$ of −0.62‰ during this part of the Oligocene, and bottom water temperatures that fluctuated in the range of ∼1–6°C.

[51] The 0.19 to 0.23‰ change during the Oi events that are not related to ice volume (section 4.8) would then be attributed to deep sea temperature changes of 0.76 to 0.92°C (with ∼0.25‰°C [*Epstein et al.*, 1953]). In the planktonic foraminiferal record changes in $\delta^{18}O$ ascribed to temperature range between 0.20 and 1.72°C. The largest change

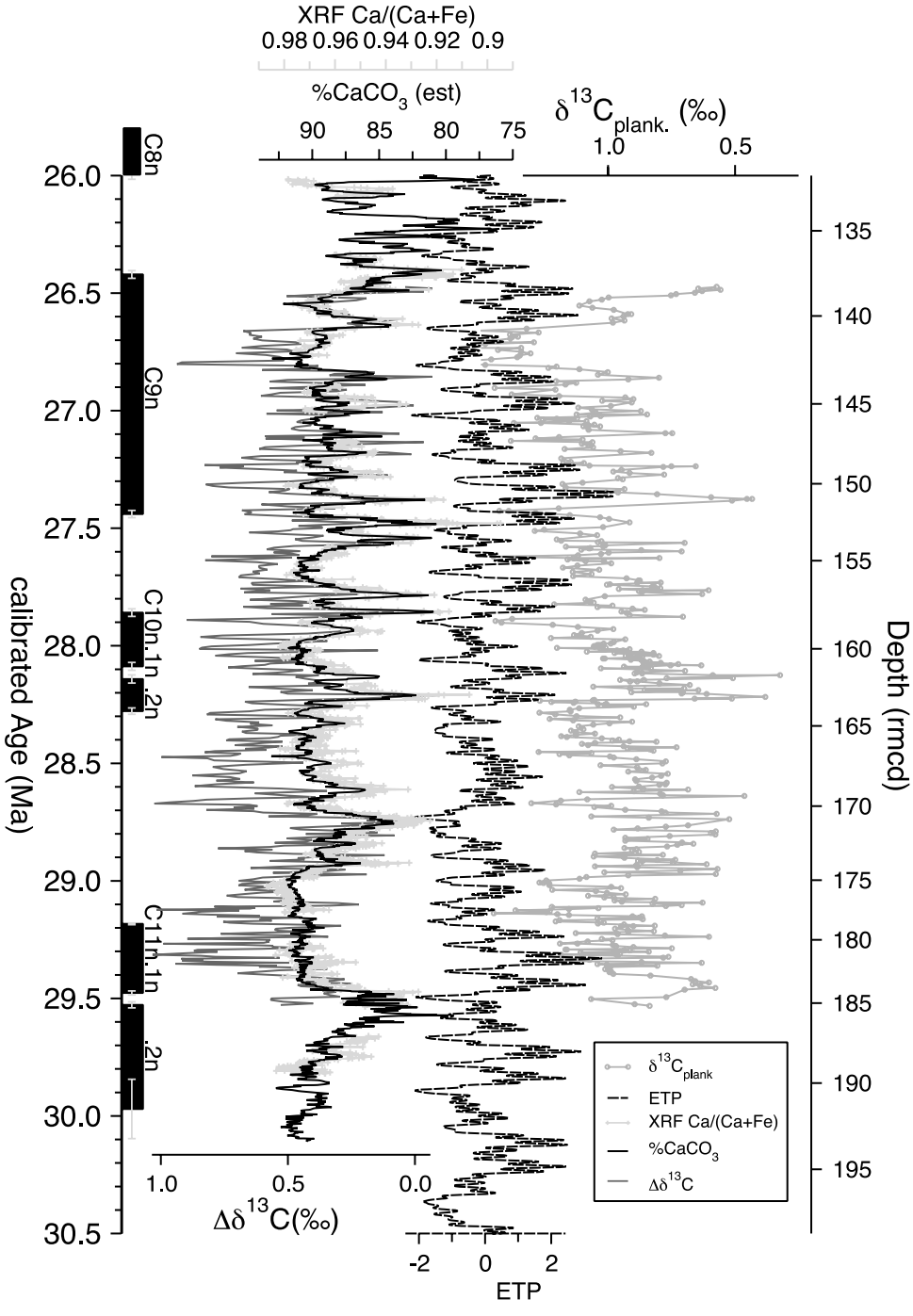

Figure 8. Planktonic foraminifera carbon isotopes and benthic-planktonic carbon isotope difference from Site 1218, against calculated percent $CaCO_3$ and Ca, Fe XRF measurements. Note the very close correspondence of carbonate contents and $\Delta\delta^{13}C$. See color version of this figure in the HTML.

occurs around Oi-2a (70_{Ol}), where planktonic foraminiferal oxygen isotope values shift by 1.01‰ (Table 1).

4.11. Oligocene $\delta^{13}C$ Variations and the Carbon Cycle

[52] Enriched $\delta^{18}O$ values and eustatic fall during the Oi events are associated with positive $\delta^{13}C$ excursions in benthic foraminifera (Figure 2). The magnitude and cyclicity of the carbon isotope shifts is similar to that recorded in carbon isotope records of the Oligocene and Miocene [*Miller and Fairbanks*, 1985; *Pisias et al.*, 1985; *Woodruff and Savin*, 1991; *Flower and Kennett*, 1993; *Zachos et al.*, 1996; *Paul et al.*, 2000; *Zachos et al.*, 2001b], suggesting that this climatic regime is consistent for at least 10 million years.

[53] The high-resolution data from Site 1218 indicate that substantial, pronounced (1‰) oscillations in $\delta^{13}C$ are also

reflected in the planktonic foraminifera and $\Delta\delta^{13}C$ records. Heavy planktonic foraminifera $\delta^{13}C$ values (>1.4‰) and enhanced carbon isotope gradients are recorded at 29.1, 27.9 and 26.8 Ma, associated with the Oi events (Figure 4). This indicates that the carbon isotope variations were a global signal and influenced the entire water column.

[54] These increases in planktonic foraminifera $\delta^{13}C$ match cycles within the lithological record and are associated with increased percent carbonate (Figure 8). The significant cyclic variations in $\delta^{13}C$ and $CaCO_3$ content may reflect either changes in carbonate export productivity or alternatively a secondary effect of dissolution/diagenesis. While diagenesis has been shown to influence the $\delta^{18}O$ of planktonic foraminifera [*Pearson et al.*, 2001] and limited empirical evidence exists to explain high-amplitude changes in planktonic foraminifera $\delta^{13}C$ through diagenesis and the carbonate ion effect [*Spero et al.*, 1997; *Zeebe et al.*, 1999; *Russell and Spero*, 2000], the influence of diagenesis on the $\delta^{13}C$ signal of planktonic foraminifera appears to be negligible. Foraminifera and calcareous nannofossils are still abundant during lower (80%) carbonate intervals, and samples contain a full assemblage of Oligocene planktonic foraminiferal fauna.

[55] Significant and coherent variation at short and long-term eccentricity frequencies are prevalent in $\delta^{13}C$ records (Figure 5) and $\%CaCO_3$ records. The cyclic $\delta^{13}C$ gradient between planktonic and benthic foraminifera has considerable implications regarding the nature of carbon burial during the Oligocene. Orbital forcing and particularly modulation by the eccentricity cycles affected both export productivity and carbon burial.

[56] The association and cyclic variations of $\delta^{13}C$ in planktonic and benthic foraminifera, enhanced $\Delta\delta^{13}C$ and increased carbonate content during each of the glacial events is significant. Increases in the water column carbon isotope gradient are also documented during Pleistocene glaciations [*Hodell et al.*, 2003]. This suggests a direct relationship between the carbon cycle and glaciations, and supports the oscillation of the carbon cycle and pCO_2 levels in relation to ice sheet development and expansion. Enhanced productivity and an increased rate of burial of organic carbon during glacial events would account for the high-amplitude $\delta^{13}C$ variations. Glacioeustatic sea level fall during Oi events may have increased continental weathering rates, and ocean eutrophication by revealing and eroding nutrient rich sediments on the continental shelf and transferring them to the ocean.

[57] Previous studies have suggested that the increased benthic foraminifera $\delta^{13}C$ values during the Oi events are related to changes in the deep sea carbon reservoir and enhanced organic carbon burial [*Miller and Fairbanks*, 1985; *Woodruff and Savin*, 1991; *Paul et al.*, 2000]. While previous studies demonstrated a very strong response of benthic $\delta^{13}C$ values on eccentricity timescales during the late Oligocene [*Zachos et al.*, 2001b; *Billups et al.*, 2002], additional information about the link between the global carbon budget has been provided by studies from earlier times during in the Eocene and Paleocene. In particular, *Cramer et al.* [2003] described a sequence of re-occurring light $\delta^{13}C$ events during eccentricity (and thus climatic precession amplitude) maxima. They proposed a model that simulates the shape of carbon isotope curves very well as a nonlinear response of the carbon budget to astronomical forcing, and which explains the strong response at timescales >0.1 Myr by the residence time of carbon in the oceans [*Cramer*, 2003].

[58] While the substantial shifts and maxima in the planktonic foraminifer $\delta^{13}C$ record and increased $\delta^{13}C$ gradient between the surface and the deep ocean are to a large extent attributed to the global carbon reservoir signal, the planktonic carbon record reveal much more pronounced short-term eccentricity variations (110 kyr). The corresponding changes in percent carbonate and increases in planktonic foraminiferal $\delta^{13}C$ suggest an enhanced production of biogenic material and mass accumulation rates related to changes in surface water productivity. Indeed, strongly changing productivity patterns and advective flow of eutrophic waters in the area have been suggested by sediment mass accumulation rate studies for the Pacific equatorial region, with a pattern of productivity that was quite different to the single upwelling driven equatorial belt that we see at present [*Moore et al.*, 2004]. Cyclic shifts in the boundary between the North Equatorial Current and the Equatorial Counter Current, related to orbital modulation of wind patterns may account for changes in surface water productivity.

5. Summary and Conclusion

[59] We presented stable isotope data from both planktonic and benthic foraminifera from ODP Site 1218 at a ~6 kyr resolution that provide a detailed, continuous, 3.6 Myr record of climate and paleoceanographic change in the equatorial Pacific during the Oligocene. Together with additional collaborative studies from the earlier and later Oligocene, they will form part of a Pacific stable isotope reference section. Increases in both planktonic and benthic foraminifera $\delta^{18}O$ are used to constrain the magnitude and timing of major fluctuations in ice volume and global sea level change. Glacial episodes, modulated by obliquity and eccentricity frequencies, occurred at 29.16, 27.91 and 26.76 Ma. These correspond to glacioeustatic sea level fluctuations of 50 to 65 m. High amplitude cyclic variations are recorded in the carbon isotope signal of planktonic and benthic foraminifera, the water column carbon isotope gradient and estimated percent carbonate. Maxima in $\delta^{13}C$ and the increased $\Delta\delta^{13}C$ values are associated with each of the glacial events. Alteration of high-latitude temperatures and Antarctic ice volume thus had a significant impact on the global carbon burial and equatorial productivity. During the Oligocene ice volume and temperature variations were driven by the 405 kyr and 1.2 Myr orbital cycles, which exerted a prominent influence on climate, equatorial productivity and global sea level changes, and allows the development of a new astronomical cycle based naming scheme.

[60] **Acknowledgments.** We are grateful for the reviews of J. Zachos and M. Huber. We thank H. Brinkhuis, J. Zachos, J. Backman, P. Pearson and J. Herrle for discussions, C. Chilcott for mass spectrometer assistance at the University of Edinburgh and R. Hesketh and K. Marsden for help with

sample preparation, and K. Hajnal, P. Torssander and Å. Wallin for help with benthic isotope measurements and sample preparation in Stockholm. This research used samples provided by the Ocean Drilling Program (ODP). ODP is sponsored by the U.S. National Science Foundation and participating countries under the management of Joint Oceanographic Institutions, Inc. Financial support was provided by the Swedish Research Council and the UK Natural Environment Research Council (NERC) to H.P., and by NERC (reference NER/I/S/2000/00954) and a Rapid Response Award from UK ODP to B.S.W. XRF measurements were obtained at Bremen University with funding through the European Paleostudies programme.

References

Aubry, M.-P. (1992), Paleogene calcareous nannofossils from the Kerguelen Plateau, Leg 120, *Proc. Ocean Drill. Program Sci. Results*, *120*, 471–491.

Billups, K., J. E. T. Channell, and J. C. Zachos (2002), Late Oligocene to early Miocene geochronology and paleoceanography from the subantarctic South Atlantic, *Paleoceanography*, *17*(1), 1004, doi:10.1029/2000PA000568.

Billups, K., H. Pälike, J. E. T. Channell, J. C. Zachos, and N. J. Shackleton (2004), Astronomical calibration of the late Oligocene through early Miocene geomagnetic polarity time scale, *Earth Planet. Sci. Lett.*, *224*(1–2), 33–44.

Biolzi, M. (1983), Stable isotopic study of Oligocene-Miocene sediments from DSDP Site 354, equatorial Atlantic, *Mar. Micropaleontol.*, *8*(2), 121–139, doi:10.1016/0377-8398(83)90008-7.

Browning, J. V., K. G. Miller, and D. K. Pak (1996), Global implications of lower to middle Eocene sequence boundaries on the New Jersey coastal plain; the icehouse cometh, *Geology*, *24*(7), 639–642, doi:10.1130/0091-7613(1996)024<0639:GIOLTM>2.3.CO;2.

Cande, S. C., and D. V. Kent (1995), Revised calibration of the geomagnetic polarity timescale for the late Cretaceous and Cenozoic, *J. Geophys. Res.*, *100*(B4), 6093–6095.

Coxall, H. K., P. A. Wilson, H. Pälike, C. H. Lear, and J. Backman (2004), Rapid stepwise onset of Antarctic glaciation and deeper calcite compensation in the Pacific Ocean, *Nature*, in press.

Cramer, B. S. (2003), Deconvolving the carbon isotope record, *Eos Trans. AGU*, *84*(46), Fall Meet. Suppl., Abstract B11B–07.

Cramer, B. S., J. D. Wright, D. V. Kent, and M.-P. Aubry (2003), Orbital climate forcing of $\delta^{13}C$ excursions in the late Paleocene–early Eocene (chrons C24n–C25n), *Paleoceanography*, *18*(4), 1097, doi:10.1029/2003PA000909.

Douglas, R. G., and S. M. Savin (1978), Oxygen isotopic evidence for the depth stratification of Tertiary and Cretaceous planktic foraminifera, *Mar. Micropaleontol.*, *3*(2), 175–196.

Duplessy, J. C., C. Lalou, and A. C. Vinot (1970), Differential isotopic fractionation in benthic foraminifera and palaeotemperatures reassessed, *Science*, *168*(3928), 250–251.

Epstein, S., R. Buchsbaum, H. A. Lowenstamm, and H. C. Urey (1953), Revised carbonate-water isotopic temperature scale, *Geol. Soc. Am. Bull.*, *64*, 1315–1326.

Erez, J., and B. Luz (1983), Experimental palaeotemperature equation for planktonic foraminifera, *Geochim. Cosmochim. Acta*, *47*(6), 535–538, doi:10.1016/0016-7037(83)90232-6.

Fairbanks, R. G. (1989), A 17,000-year glacio-eustatic sea-level record: Influence of glacial melting rates on the Younger Dryas Event and deep-ocean circulation, *Nature*, *342*(6250), 637–642, doi:10.1038/342637a0.

Fairbanks, R. G., and R. K. Matthews (1978), The marine oxygen isotope record in Pleistocene coral, Barbados, West Indies, *Quat. Res.*, *10*, 181–196.

Flower, B. P., and J. P. Kennett (1993), Middle Miocene ocean-climate transition: High-resolution oxygen and carbon isotopic records from Deep Sea Drilling Project Site 588A, southwest Pacific, *Paleoceanography*, *8*(6), 811–843.

Gale, A. S., J. Hardenbol, B. Hathway, W. J. Kennedy, J. R. Young, and V. Phansalkar (2002), Global correlation of Cenomanian (Upper Cretaceous) sequences: Evidence for Milankovitch control, *Geology*, *30*(4), 291–294, doi:10.1130/0091-7613(2002)030<0291:GCOCUC>2.0.CO;2.

Gasperi, J. T., and J. P. Kennett (1993), Miocene planktonic foraminifers at DSDP Site 289; depth stratification using isotopic differences, *Proc. Ocean Drill. Program Sci. Results*, *130*, 323–332.

Ghil, M., et al. (2002), Advanced spectral methods for climatic time series, *Rev. Geophys.*, *40*(1), 1003, doi:10.1029/2000RG000092.

Gibbs, S. J., N. J. Shackleton, and J. Young (2004), Orbitally forced climate signals in mid-Pliocene nannofossil assemblages, *Mar. Micropaleontol.*, *51*, 39–56, doi:10.1016/j.marmicro.2003.09.002.

Haq, B. U. (1980), Biogeographic history of Miocene calcareous nannoplankton and paleoceanography of the Atlantic Ocean, *Micropaleontology*, *26*(4), 414–443.

Haq, B. U., and G. P. Lohmann (1976), Early Cenozoic calcareous nannoplankton biogeography of the Atlantic Ocean, *Mar. Micropaleontol.*, *1*(2), 119–194.

Haq, B., J. Hardenbol, and P. Vail (1987), Chronology of fluctuating sea levels since the Triassic, *Science*, *235*, 1156–1167.

Hardenbol, J. (2003), Paleogene Sequence Chronostratigraphy, in *ISPS Symposium on the Paleogene: Preparing for Modern Life and Climate*, *Proceedings with Abstracts*, pp. S5–S6, Leuven, Belgium.

Hodell, D. A., K. A. Venz, C. D. Charles, and U. S. Ninnemann (2003), Pleistocene vertical carbon isotope and carbonate gradients in the South Atlantic sector of the Southern Ocean, *Geochem. Geophys. Geosys.*, *4*(1), 1004, doi:10.1029/2002GC000367.

Keigwin, L., and G. Keller (1984), Middle Oligocene cooling from equatorial Pacific DSDP Site 77B, *Geology*, *12*, 16–19.

Kominz, M. A., and S. F. Pekar (2001), Oligocene eustasy from two-dimensional sequence stratigraphic backstripping, *Geol. Soc. Am. Bull.*, *113*, 291–304, doi:10.1130/0016-7606(2001)113<0291:OEFTDS>2.0.CO;2.

Laskar, J. (1999), The limits of Earth orbital calculations for geological time-scale use, *Philos. Trans. R. Soc. London, Ser. A*, *357*(1757), 1735–1759, doi:10.1098/rsta.1999.0399.

Laskar, J., F. Joutel, and F. Boudin (1993), Orbital, precessional, and insolation quantities for the Earth from −20 Myr to +10 Myr, *Astron. Astrophys.*, *270*(1–2), 522–533, doi:10.1051/0004-6361:20035710.

Laskar, J., M. Gastineau, F. Joutel, P. Robutel, B. Levrard, and A. Correia (2004a), Long term evolution and chaotic diffusion of the insolation quantities of Mars, *Icarus*, *170*(2), 343–364, doi:10.1016/j.icarus.2004.04.005.

Laskar, J., P. Robutel, F. Joutel, M. Gastineau, A. Correia, and B. Levrard (2004b), A long term numerical solution for the insolation quantities of the Earth, *Astron. Astrophys.*, preprint. (Available from http://hal.ccsd.cnrs.fr/ccsd-00001603)

Lear, C. H., Y. Rosenthal, H. K. Coxall, and P. A. Wilson (2004), Late Eocene to early Miocene ice sheet dynamics and the global carbon cycle, *Paleoceanography*, *19*, PA4015, doi:10.1029/2004PA001039.

Lohmann, G. P., and J. J. Carlson (1981), Oceanographic significance of Pacific late Miocene calcareous nannoplankton, *Mar. Micropaleontol.*, *6*, 553–579, doi:10.1016/0377-8398(81)90021-9.

Lourens, L. J., and F. J. Hilgen (1997), Long-periodic variations in the Earth's obliquity and their relation to third-order eustatic cycles and Late Neogene glaciations, *Quat. Int.*, *40*, 43–52, doi:10.1016/S1040-6182(96)00060-2.

Miller, K. G., and R. G. Fairbanks (1985), Oligocene to Miocene carbon isotope cycles and abyssal circulation changes, in *The Carbon Cycle and Atmospheric CO_2: Natural Variations Archean to Present*, *Geophys. Monogr. Ser.*, vol. 32, edited by T. Sundquist Eric and S. Broecker Wallace, pp. 469–486, AGU, Washington, D. C.

Miller, K. G., R. G. Fairbanks, and G. S. Mountain (1987), Tertiary oxygen isotope synthesis, sealevel history, and continental margin erosion, *Paleoceanography*, *2*, 1–19.

Miller, K. G., J. D. Wright, and R. G. Fairbanks (1991), Unlocking the Ice House—Oligocene-Miocene oxygen isotopes, eustasy, and margin erosion, *J. Geophys. Res.*, *96*(B4), 6829–6848.

Miller, K. G., and G. S. Mountain, the LEG 150 Shipboard Party, and Members of the New Jersey Coastal Plain Drilling Project (1996), Drilling and dating New Jersey Oligocene-Miocene sequences: Ice volume, global sea level, and Exxon records, *Science*, *271*(5252), 1092–1095.

Miller, K. G., G. S. Mountain, J. V. Browning, M. Kominz, P. J. Sugarman, N. Christie-Blick, M. E. Katz, and J. D. Wright (1998), Cenozoic global sea level, sequences, and the New Jersey transect: Results from coastal plain and continental slope drilling, *Rev. Geophys.*, *36*(4), 569–601.

Moore, T. C., Jr., J. Backman, I. Raffi, C. Nigrini, A. Sanfilippo, H. Plike, and M. Lyle (2004), Paleogene tropical Pacific: Clues to circulation, productivity, and plate motion, *Paleoceanography*, *19*, PA3013, doi:10.1029/2003PA000998.

Paillard, D., L. Labeyrie, and P. Yiou (1996), Macintosh program performs time-series analysis, *Eos Trans. AGU*, *77*, 379.

Pälike, H., J. Laskar, and N. J. Shackleton (2004), Geologic constraints on the chaotic diffusion of the solar system, *Geology*, *32*(11), 929–932, doi:10.1130/G20750.1.

Paul, H. A., J. C. Zachos, B. P. Flower, and A. Tripati (2000), Orbitally induced climate

and geochemical variability across the Oligocene/Miocene boundary, *Paleoceanography*, *15*(5), 471–485.

Pearson, P. N., N. J. Shackleton, and M. A. Hall (1993), Stable isotope paleoecology of Middle Eocene planktonic foraminifera and multi-species isotope stratigraphy, DSDP Site 523, South Atlantic, *J. Foraminiferal Res.*, *23*(2), 123–140.

Pearson, P., P. W. Ditchfield, J. Singano, K. G. Harcourt-Brown, C. J. Nicholas, R. K. Olsson, N. J. Shackleton, and M. A. Hall (2001), Warm tropical sea surface temperatures in the late Cretaceous and Eocene epochs, *Nature*, *413*(6855), 481–487, doi:10.1038/35097000.

Pekar, S., and K. G. Miller (1996), New Jersey Oligocene "Icehouse" sequences (ODP Leg 150X) correlated with global $\delta^{18}O$ and Exxon eustatic records, *Geology*, *24*(6), 567–570, doi:10.1130/0091-7613(1996)024<0567:NJOISO>2.3.CO;2.

Pekar, S. F., K. G. Miller, and M. A. Kominz (2000), Reconstructing the stratal geometry of latest Eocene to Oligocene sequences in New Jersey: resolving a patchwork distribution into a clear pattern of progradation, *Sediment. Geol.*, *134*, 93–109, doi:10.1016/S0037-0738(00)00015-4.

Pekar, S. F., N. Christie-Blick, M. A. Kominz, and K. G. Miller (2001), Evaluating the stratigraphic response to eustasy from Oligocene strata in New Jersey, *Geology*, *29*(1), 55–58, doi:10.1130/0091-7613(2001)029<0055:ETSRTE>2.0.CO;2.

Pekar, S. F., N. Christie-Blick, M. A. Kominz, and K. G. Miller (2002), Calibration between eustatic estimates from backstripping and oxygen isotopic records for the Oligocene, *Geology*, *30*(10), 903–906, doi:10.1130/0091-7613(2002)030<0903:CBEEFB>2.0.CO;2.

Perch-Nielsen, K. (1985), Cenozoic calcareous nannofossils, in *Plankton Stratigraphy*, edited by M. Bolli Hans, B. Saunders John, and K. Perch-Nielsen, pp. 427–554, Cambridge Univ. Press, New York.

Pisias, N. G., N. J. Shackleton, and M. A. Hall (1985), Stable isotope and calcium carbonate records from hydraulic piston cored hole 574A: High-resolution records from the middle Miocene, *Initial Rep. Deep Sea Drill. Project, 85*, edited by L. A. Mayer et al., pp. 735–748, U.S. Govt. Print. Off., Washington, D. C.

Russell, A. D., and H. J. Spero (2000), Field examination of the oceanic carbonate ion effect on stable isotopes in planktonic foraminifera, *Paleoceanography*, *15*, 43–52.

Schrag, D. P., D. J. DePaolo, and F. M. Richter (1992), Oxygen isotope exchange in a two-layer model of oceanic crust, *Earth Planet. Sci. Lett.*, *111*(2–4), 305–317, doi:10.1016/0012-821X(92)90186-Y.

Schrag, D. P., D. J. DePaolo, and F. M. Richter (1995), Reconstructing past sea surface temperatures: Correcting for diagenesis of bulk marine carbonate, *Geochim. Cosmochim. Acta*, *59*(11), 2265–2278, doi:10.1016/0016-7037(95)00105-9.

Schulz, M., and M. Mudelsee (2002), REDFIT: Estimating red-noise spectra directly from unevenly spaced paleoclimatic time series, *Comput. Geosci.*, *28*(3), 421–426, doi:10.1016/S0098-3004(01)00044-9.

Shackleton, N. J. (1986), Palaeogene stable isotope events, *Palaeogeogr. Palaeoclimatol. Palaeoecol.*, *57*, 91–102, doi:10.1016/0031-0182(86)90008-8.

Shackleton, N. J., and N. D. Opdyke (1973), Oxygen isotope and palaeomagnetic stratigraphy of equatorial Pacific Core V28-238: Oxygen isotope temperatures and ice volumes on a 105 and 106 year scale, *Quat. Res.*, *3*(1), 39–55.

Shackleton, N. J., S. J. Crowhurst, G. P. Weedon, and J. Laskar (1999a), Astronomical calibration of Oligocene-Miocene time, *Philos. Trans. R. Soc. London, Ser. A*, *357*(1757), 1907–1929, doi:10.1098/rsta.1999.0407.

Shackleton, N. J., I. N. McCave, and G. P. Weedon (1999b), Preface to Astronomical (Milankovitch) calibration of the geological time-scale: A discussion meeting held at the Royal Society on 9 and 10 December 1998, *Philos. Trans. R. Soc. London, Ser. A*, *357*(1757), 1733–1734, doi:10.1098/rsta.1999.0398.

Shackleton, N. J., M. A. Hall, I. Raffi, L. Tauxe, and J. Zachos (2000), Astronomical calibration age for the Oligocene/Miocene boundary, *Geology*, *28*(5), 447–450, doi:10.1130/0091-7613(2000)028<0447:ACAFTO>2.3.CO;2.

Shipboard Scientific Party (2002), Site 1218, *Proc. Ocean Drill. Project, Initial Rep., 199*, 1–125. (Available at http://www-odp.tamu.edu/publications/199_IR/199toc.htm.)

Spero, H. J., J. Bijma, D. W. Lea, and B. E. Bemis (1997), Effect of seawater carbonate concentration on foraminiferal carbon and oxygen isotopes, *Nature*, *390*(6659), 497–500.

Turco, E., F. J. Hilgen, L. J. Lourens, N. J. Shackleton, and W. J. Zachariasse (2001), Punctuated evolution of global climate cooling during the late midddle to early late Miocene: High-resolution planktonic foraminiferal and oxygen isotope records from the Mediterranean, *Paleoceanography*, *16*(46), 405–423.

van Eijden, A. J. M., and G. M. Ganssen (1995), An Oligocene multi-species foraminiferal oxygen and carbon isotope record from ODP Hole 758A (Indian Ocean): Paleoceanographic and paleo-ecologic implications, *Mar. Micropaleontol.*, *25*, 47–65, doi:10.1016/0377-8398(94)00028-L.

Wade, B. S., and H. Pälike (2004), Data report: Oligocene paleoceanography of the equatorial Pacific, Planktonic and benthic stable isotope results from site 1218, *Proc. Ocean Drill. Program Sci. Results*, *199*, in press.

Woodruff, F., and S. M. Savin (1991), Mid-Miocene isotope stratigraphy in the deep sea; high-resolution correlations, paleoclimatic cycles, and sediment preservation, *Paleoceanography*, *6*(6), 755–806.

Wright, J. D., K. G. Miller, and R. G. Fairbanks (1992), Early and middle Micocene stable isotopes: Implications for deepwater circulation and climate, *Paleoceanography*, *7*, 357–389.

Zachos, J. C., T. M. Quinn, and K. A. Salamy (1996), High resolution (104 years) deep-sea foraminiferal stable isotope records of the Eocene-Oligocene climate transition, *Paleoceanography*, *11*(3), 251–266.

Zachos, J. C., M. Pagani, L. Sloan, E. Thomas, and K. Billups (2001a), Trends, rhythms, and aberrations in global climate 65 Ma to present, *Science*, *292*(5517), 686–693, doi:10.1126/science.1059412.

Zachos, J. C., N. J. Shackleton, J. S. Revenaugh, H. Pälike, and B. P. Flower (2001b), Climate response to orbital forcing across the Oligocene-Miocene Boundary, *Science*, *292*(5515), 274–278, doi:10.1126/science.1058288.

Zeebe, R. E., J. Bijma, and D. A. Wolf-Gladrow (1999), A diffusion-reaction model of carbon isotope fractionation in foraminifera, *Mar. Chem.*, *64*(3), 199–227, doi:10.1016/S0304-4203(98)00075-9.

H. Pälike, Southampton Oceanography Centre, School of Ocean and Earth Science, European Way, Southampton SO14 3ZH, UK. (heiko.palike@soc.soton.ac.uk)

B. S. Wade, School of Earth, Ocean and Planetary Sciences, Cardiff University, Main Building, Park Place, Cardiff CF10 3YE, UK. (wadeb2@cardiff.ac.uk)